FULL TITLE
ASP Conference Series, Vol. **VOLUME**, **YEAR OF PUBLICATION**
NAMES OF EDITORS

Phenomenological Modeling of the FIR–Radio Correlation within Nearby Star-Forming Galaxies

E.J. Murphy[1], G. Helou[2], L. Armus[2], R. Braun[3], J.D.P. Kenney[1], and the SINGS team

[1] *Yale University;* [2] *Spitzer Science Center/Caltech;* [3] *ASTRON*

Abstract. We present an analysis of the far-infrared (FIR)-radio correlation within a group of nearby star-forming galaxy disks observed as part of the *Spitzer* Infrared Nearby Galaxies Survey (SINGS). In our study we critically test a phenomenological model for the FIR-radio correlation which describes the radio image as a smeared version of the infrared image. The physical basis for this model is that cosmic-ray electrons (CR electrons) will diffuse significant distances from their originating sources before decaying by synchrotron emission. We find that this description generally works well, improving the correlation between the radio and infrared images of our four sample galaxies by an average factor of ∼1.6. We also find that the best-fit smearing kernels seem to show a dependence on the ongoing star formation activity within each disk. Galaxies having lower star formation activity (NGC 2403 and NGC 3031) are best-fit using larger smearing kernels than galaxies with more active star-forming disks (NGC 5194 and NGC 6946). We attribute this trend to be due to a recent deficit of CR electron injection into the interstellar medium of galaxies with lower star formation activity throughout their disks.

1. Introduction

The near-universality of the far-infrared (FIR)–radio correlation lends it to be a critical tool for constraining the physical processes that shape galaxies. While the FIR-radio correlation can teach us how the global parameters of galaxies work with one another to keep the integrated thermal dust emission in constant proportion with the non-thermal radio synchrotron emission, resolved studies can help us understand the link between relativistic and non-relativistic phases of the interstellar medium (ISM) on a much more intimate level.

To date, nearly all of our observational knowledge about the relativistic phase (cosmic-ray component) of the ISM comes from direct measurements of cosmic-ray (CR) nuclei in the solar neighborhood. These observational characteristics of the CR component of the Galaxy are normally considered to be applicable for all galaxies. The only observational constraints on CR physics in other galaxies comes from multi-wavelength radio observations which are able to probe the CR electron component of galaxies (eg. Lisenfeld et al. (1996)). However, these data alone only describe the present distribution of CR electrons without providing insight on the CR electron source distribution and, consequently, the diffusion and propagation history of the CR electrons.

Previous studies of the FIR-radio correlation using *IRAS* data have tried to explain it using a phenomenological model in which the radio image appears as

a smeared version of the infrared image (Bicay & Helou 1990; Marsh & Helou 1998). The physical backing of this picture arises from the fact that CR electrons diffuse much larger distances (∼1-2 kpc) compared to the mean free path of dust heating UV photons (∼100 pc). Murphy et al. (2006) have recently shown that the correlation between the FIR and radio emission within galaxies on sub-kpc scales displays a non-linearity with FIR/radio ratio increasing with FIR surface brightness. This non-linearity can be attributed to the diffusion of CR electrons away from star-formation sites in agreement with the 'image-smearing' picture. In this conference proceedings, we highlight the results of the phenomenological 'image-smearing' model when applied to a sample of four nearby star-forming galaxies (NGC 2403, NGC 3031, NGC 5194, and NGC 6946) using *Spitzer* MIPS and WSRT radio continuum data, observed as part of the *Spitzer* Nearby Galaxies Survey (SINGS) (Kennicutt et al. 2003). These galaxies display a range in their star formation activity and Hubble types, but are at distances that allow us to study the correlation on sub-kpc scale.

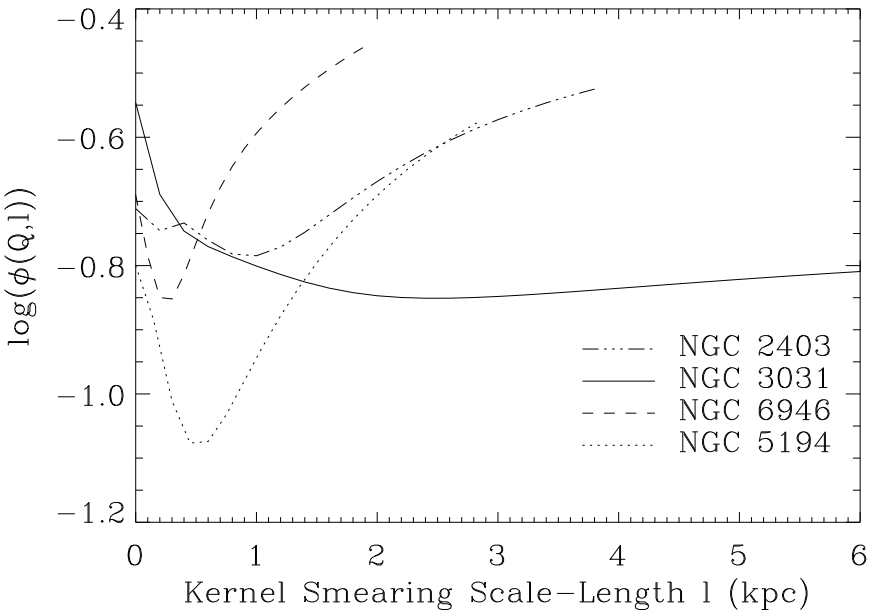

Figure 1. Residuals between the smeared 70 μm and radio maps are plotted as a function of the smearing kernel scale-length for each of the four sample galaxies. Notice the different behavior among the residual curves. Residual curves for galaxies with higher star formation activity (NGC 5194 and NGC 6946) display narrow troughs with well defined minima. The less active star-forming galaxies (NGC 2403 and NGC 3031) have much broader troughs with less well defined minima. NGC 2403 even shows evidence for two minima at ∼0.2 and ∼1.0 kpc which may be the result of a superposition of two distinct CR electron populations having significantly different ages.

2. Results

In Figure 1 we plot the residuals between the smoothed 70 μm and radio maps against the scale-length (l) of the smearing kernel. The 70 μm images are smoothed by exponential kernels projected in the plane of the sky which take the form $\kappa(\mathbf{r}) = e^{-r/l}$. A comparison of the residual curves among the four sample galaxies shows a range in behavior and a factor of $\sim$1.6 mean improvement in the correlation. NGC 5194 and NGC 6946 both have well behaved residual curves, displaying rather narrow troughs with well defined minima corresponding to smearing scale-lengths less than 1 kpc. NGC 2403 and NGC 3031, on the other hand, exhibit different behavior. The residual curve for NGC 3031 is very shallow and has a minimum centered around $\sim$2.5 kpc that is not well constrained. In the case of NGC 2403, we see evidence for two minima in its residual curve. The first minimum corresponds to a smearing scale-length of $\sim$0.2 kpc, while the second, and deeper of the two, occurs for a scale-length around $\sim$1.0 kpc.

In Figure 2 we plot the residual maps associated with the best-fit smearing kernel. For each galaxy we find non-noiselike residuals displaying organized structure co-spatial with areas of star formation. We also find distinct and opposite behavior in the residual maps of NGC 2403 and NGC 3031 when compared with those for NGC 5194 and NGC 6946. While NGC 2403 and NGC 3031 display radio excesses in their residual maps associated with sites of star formation, NGC 5194 and NGC 6946 exhibit infrared excesses around star-forming regions. This is not surprising since galaxies best fit with large smearing kernels have increased amounts of flux redistributed away from bright star-forming regions which will result in radio excesses for these locations in the residual maps.

3. Discussion

Using new high resolution *Spitzer* imaging at 70 μm for a sample of 4 galaxies, we have applied a phenomenological model for the FIR-radio correlation, which describes the distribution of radio emission as a smoother version of the infrared flux distribution. We find that the model fitting parameters seem to differ depending on the amount of ongoing star formation activity within each galaxy.

While we see dramatically different residual behavior for NGC 5194 and NGC 6946 compared to NGC 2403 and NGC 3031, we also find that these pairs of galaxies have quite different ongoing star formation within their disks. Both NGC 5194 and NGC 6946 have star-formation rates (SFRs) which are roughly a factor of $\sim$6 higher than NGC 2403 and NGC 3031 (Murphy et al. 2006). We attribute the differences in the residuals among the four galaxies to be due to timescale effects. In the less active star-forming galaxies there has likely been a deficit of recent CR electron injection into their ISM leaving the diffuse disk as the dominant morphological structure. Accordingly, in the more active star-forming galaxies, CR electrons are likely being injected into the ISM at a much higher rate, thereby keeping both the mean age of the CR electron distribution young and their mean diffusion lengths short. We speculate the double minima behavior for the residual curve of NGC 2403 to be due to a superposition of two distinct CR electron populations having significantly different ages.

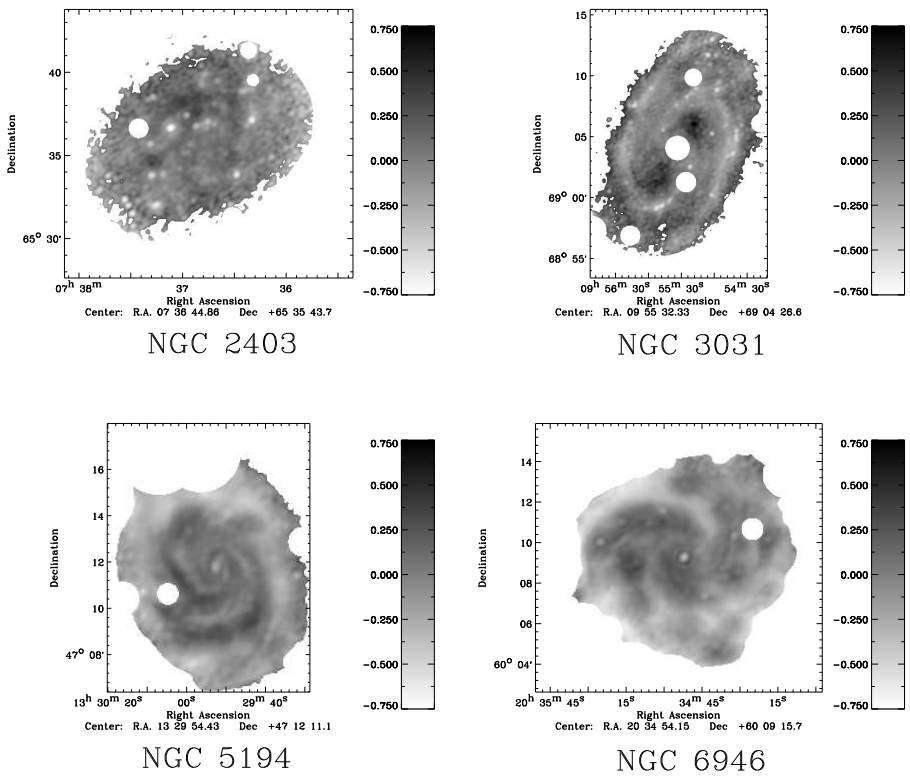

Figure 2. Residual images after subtracting the observed radio maps from the smeared 70 μm images for each galaxy using the best-fit exponential kernel oriented in the plane of the sky. Notice the non-noiselike residuals left behind which seem to vary from one galaxy to the next. The residual maps for galaxies with higher star formation activity (NGC 5194 and NGC 6946) display infrared excess associated with star formation sites. Galaxies with lower star formation activity (NGC 2403 and NGC 3031) display an opposite trend in which star formation sites exhibit radio excesses due to a large smearing kernel.

Acknowledgments. E.J.M. would like to acknowledge support provided by the *Spitzer* Science Center Visiting Graduate Student program. As part of the *Spitzer* Space Telescope Legacy Science Program, support was provided by NASA through Contract Number 1224769 issued by the Jet Propulsion Laboratory, California Institute of Technology under NASA contract 1407.

References

Bicay M. D. and Helou, G. 1990, ApJ, 362, 59
Kennicutt, R. C. Jr., et al. 2003, PASP, 115, 928
Lisenfeld, U., Alexander, P., Pooley, G. G., and Wilding, T. 1996, MNRAS, 281, 301
Marsh, K. A. and Helou, G. 1998, ApJ, 493, 121
Murphy E. J., et al. 2006, ApJ, 638, 157